Environ. Sci. Technol. **1997**, *31*, 1345−1358

Secondary Organic Aerosol from the Photooxidation of Aromatic Hydrocarbons: Molecular Composition

HALI J. L. FORSTNER, RICHARD C. FLAGAN, AND JOHN H. SEINFELD*

Department of Chemical Engineering, California Institute of Technology, Pasadena, California 91125

Outdoor smog chamber photooxidations to determine the molecular composition of secondary organic aerosol (SOA) from toluene, *m*-xylene, *p*-xylene, ethylbenzene, *m*-ethyltoluene, *p*-ethyltoluene, and 1,2,4-trimethylbenzene in sunlight-irradiated hydrocarbon−NO_x mixtures are reported. Gas-phase mechanisms leading to the observed products are proposed. Unsaturated anhydrides (2,5-furandione, 3-methyl-2,5-furandione, 3-ethyl-2,5-furandione) are predominant components of aerosol from all the aromatics, an observation that is consistent with gas-phase aromatic mechanisms involving ring fragmentation. Saturated anhydrides were also detected in significant quantities, which could result from the hydrogenation of the furandiones in sunlight in the particle phase.

Introduction

Hydrocarbons are emitted to the troposphere from anthropogenic and biogenic sources. Anthropogenic sources comprise organics such as alkanes, alkenes, aromatics, and carbonyls, while biogenic sources include organics such as terpenes and sesquiterpenes. The atmospheric photooxidation of organics yields oxygenated and nitrated products that, depending on their properties, partition between the gas and particulate phases, resulting in secondary organic aerosol (SOA) formation. The atmospheric chemistry of larger organic compounds is sufficiently complex that a spectrum of condensable and non-condensable products form from a single hydrocarbon precursor. The recent work of Pankow (*1*, *2*) on semivolatile organic gas/particle partitioning theory and the experimental evidence of Odum *et al.* (*3*) and Forstner (*4*) establishes that vapor pressure alone does not determine to what extent a vapor species will partition into the particle phase. The organic particulate mass serves as the medium into which the gas-phase species are absorbed, and thereby the amount of organic particulate mass directly affects the gas/particle partitioning. A consequence of this is that products with relatively high vapor pressures may well exist, in part, in the particle phase.

Aromatics are particularly important constituents of urban and regional atmospheric chemistry (*5*); additionally, most have been identified as aerosol precursors (*3*, *4*, *6*−*8*). Although the initial reactions of aromatics with OH are reasonably well understood, those beyond the first few steps in the NO_x−air photooxidation remain uncertain (*9*). Typically, less than 50% of the reacted carbon has been identified in photooxidation product studies of toluene, *p*-xylene, and *m*-xylene (9). Elucidation of the photooxidation mechanisms of aromatics remains crucial for understanding their contribution to ozone and other oxidized product formation and to eventual formation of SOA (*10*). Although the focus of this work was the composition of secondary organic aerosol, it confirms first generation product identification (*9*), and in particular it corroborates the identification of dicarbonyls and anhydrides (*11*). Additional new product information for two aromatics, ethylbenzene and *p*-ethyltoluene, has been obtained. Finally, the original identification of saturated anhydrides from some aromatic precursors is suggestive of photochemically driven particle-phase hydrogenation.

* To whom correspondence should be addressed. Fax: 818-585-1729; e-mail: john@aeolus.che.caltech.edu.

TABLE 1. Initial Conditions for 1993 Outdoor Smog Chamber Experiments

aromatic	[HC] (ppm)	[C_3H_6] (ppm)	initial particles (cm^{-3})	[NO] (ppm)	[NO_2] (ppm)	HC:NO_x ratio (ppb C/ppb)
toluene	4.2	1.5	420	1.0	0.45	23
toluene	6.0	1.6	350	1.0	0.49	31
toluene	2.5	1.1	560	0.61	0.28	23
m-xylene	2.7		690	0.63	0.29	26
m-xylene	8.6	1.5	430	1.1	0.55	43
m-xylene	6.5	1.3	270	1.2	0.57	31
p-xylene	4.7	1.3	520	1.2	0.56	24
p-xylene	2.5	1.0	320	0.70	0.31	23
p-xylene	6.3	1.5	420	1.2	0.57	31

The present study represents a comprehensive effort to determine the composition of aromatic secondary aerosol. The goals are to assess aromatic photooxidation mechanisms by identifying particle-phase products and to obtain molecular product information allowing future development of quantitative prediction of SOA formation. Few studies have attempted to systematically identify components of secondary organic particles. The current study has identified species in aromatic secondary aerosol, thereby providing compelling evidence for the semivolatile organic gas/particle partitioning theory of Pankow (*1*, *2*). The identified species in the secondary organic aerosol have high vapor pressures, such that condensation as the mechanism to the particle phase is precluded. A logical mechanism by which these species can exist in the particle phase is the establishment of an equilibrium between the gas-phase concentration and the particulate organic mass concentration.

A series of outdoor smog chamber aromatic−NO_x photooxidations were performed to generate secondary organic aerosol. The aromatics studied were toluene, *m*-xylene, *p*-xylene, ethylbenzene, *m*-ethyltoluene, *p*-ethyltoluene, and 1,2,4-trimethylbenzene. After a description of the experiments and the analytical method, we summarize the particulate species identified from the above aromatics and discuss mechanisms leading to these products.

Experimental Section

Secondary Organic Aerosol Sample Generation. The 60 m^3 outdoor smog chamber facility has been described previously (*3*, *4*, *7*). Experiments were performed over the summers of 1993 and 1994. A summary of experiments performed in 1994 is given in Forstner (*4*). Initial hydrocarbon mixing ratios ranged from 200 to 900 ppb, and initial propene mixing ratios ranged from 100 to 340 ppb. Propene was added to the mixture to enhance photochemical reactivity (*7*). Initial hydrocarbon−NO_x ratios ranged from 3 to 14 ppb C/ppb, similar to those observed in the South Coast Air Basin of California (*5*). Ammonium sulfate seed aerosol was added to encourage condensation of the secondary gas-phase products. In the 1993 experiments, an 8 m^3 outdoor Teflon chamber was used (Table 1). Initial hydrocarbon mixing ratios

S0013-936X(96)00537-8 CCC: $14.00

TABLE 2. Compounds Identified in Secondary Organic Aerosol from Aromatic Photooxidation[a]

compound	toluene	*m*-xylene	*p*-xylene	1,2,4-trimethylbenzene	ethylbenzene	*m*-ethyltoluene	*p*-ethyltoluene
2'-hydroxy-5'-methylacetophenone						0.11 ± 0.06	
2,3,5-trimethyl-1,4-benzoquinone[b]				0.04 ± 0.07			
2,4-dimethylbenzaldehyde				0.76 ± 0.82			
2,4-dimethylphenol		0.24 ± 0.27		0.03 ± 0.04			
2,5-dimethyl-1,4-benzoquinone[c]			0.46 ± 0.73				
2,5-dimethylbenzaldehyde				0.46 ± 0.57			
2,5-dimethylphenol			1.9 ± 2.7	1.2 ± 1.0			
2,5-furandione	9.6 ± 1.1	5.2 ± 4.2	1.7 ± 1.3	7.0 ± 1.0	16 ± 2.1	7.4 ± 3.4	4.9 ± 0.60
2,5-heptadione							1.0 ± 1.0
2,5-hexanedione			5.6 ± 3.0			1.6 ± 0.18	1.6 ± 0.89
2,6-dimethyl-1,4-benzoquinone[b]		0.44 ± 0.40					
2,6-dimethyl-4-nitrophenol		3.3 ± 0.86					
2,6-dimethylphenol		+					
2-acetyl-5-methylfuran		4.1 ± 3.0	2.0 ± 0.99	0.26 ± 0.11	0.48 ± 0.42	0.12 ± 0.02	0.42 ± 0.24
2-ethyl-1,4-benzoquinone[b]					1.5 ± 0.42		
2-furaldehyde	0.15 ± 0.02		0.05 ± 0.06				
2-hydroxy-5-nitrobenzaldehyde	1.6 ± 1.2						
2-methyl-1,4-benzoquinone[c]	0.46 ± 0.35						
2-methyl-4,6-dinitrophenol	3.5 ± 4.0	0.39 ± 0.31					
3,4,5-trimethyl-2(3H)-furanone[d]				2.0 ± 2.2			
3,4-dimethylbenzaldehyde				0.83 ± 0.98			
3,4-dimethylbenzoic acid				12 ± 2.2			
3,4-dimethylfurandione		0.41 ± 0.36	0.19 ± 0.27	3.1 ± 1.5	0.12 ± 0.16		
3,4-dimethylphenol							+
3,4/4,5-dimethyl-2(3*H*)-furanone[d]				0.78 ± 0.25			
3,5-dimethyl-2(3*H*)-furanone[d]		0.49 ± 0.29					
3,5-dimethyl-2*H*-pyran-2-one		2.7 ± 2.1					
3-acetyl-2,5-dimethylfuran			0.32 ± 0.34	0.09 ± 0.05		1.1 ± 0.85	
3-ethyl-2(5*H*)-furanone[e]						0.42 ± 0.25	0.16 ± 0.10
3-ethyl-2,5-furandione[f]					7.4 ± 3.8	24 ± 12	35 ± 5.0
3-ethyl-5-methyl-2(3*H*)-furanone[g]						0.07 ± 0.06	
3-ethylbenzaldehyde						1.9 ± 0.81	
3-ethylbenzoic acid						6.6 ± 2.2	
3-hydroxybenzaldehyde	0.04 ± 0.05						
3'-methylacetophenone						12 ± 5.9	
3-methyl-2(5*H*)-furanone	1.4 ± 0.39	0.89 ± 0.49	1.9 ± 2.1				1.0 ± 0.35
3-methyl-2,5-furandione	26 ± 3.6	61 ± 14	53 ± 27	27 ± 0	17 ± 5.5	18 ± 6.4	16 ± 7.2
3-methyl-2,5-hexanedione[h]				9.9 ± 2.0			
3-methyl-4-nitrophenol	6.8 ± 0.80	2.1 ± 1.9					
3-methyl-5-ethyl-2(3*H*)-furanone[i]						1.3 ± 0.59	
3-methylbenzyl alcohol		0.38 ± 0.66					
3'-nitroacetophenone					1.6 ± 0.56		
3-nitrotoluene	0.18 ± 0.02		0.04 ± 0.05				
4'-hydroxy-3'-nitroacetophenone					1.5 ± 1.5		0.34 ± 0.10
4'-hydroxyacetophenone						0.52 ± 0.27	0.41 ± 0.05
4-ethylbenzaldehyde							4.0 ± 1.6
4-ethylbenzoic acid							4.7 ± 0.64
4-ethylnitrobenzene					1.8 ± 0.53		
4-hydroxy-3-methylbenzaldehyde		0.03 ± 0.06					

4'-methylacetophenone							15 ± 5.1
4-methylphthalic acid				28 ± 5.3			
4-methyl-2-nitrophenol	4.4 ± 1.4		6.0 ± 7.6				4.1 ± 1.2
4-methylbenzyl alcohol			1.8 ± 1.9				
2-methyl-4-nitro-phenol[j]	10 ± 0.12						
5-ethyl-2(3*H*)-furanone[k]					0.17 ± 0.24	1.4 ± 1.5	
5-ethyl-2-furaldehyde					3.6 ± 2.0	0.29 ± 0.51	
5-methyl-2(3*H*)-furanone	2.9 ± 1.6	3.1 ± 1.6		0.15 ± 0.13	0.62 ± 0.41	0.56 ± 0.22	0.31 ± 0.27
5-methyl-2-furancarboxaldehyde	1.6 ± 0.23		2.1 ± 2.0	1.8 ± 0.34	2.1 ± 3.0		0.91 ± 0.19
5-methylfurfural		0.84 ± 0.60					
acetophenone					19 ± 7.8	0.19 ± +	+
α-methylbenzene methanol						0.03 ± 0.06	
benzaldehyde	3.0 ± 0.46	1.4 ± 1.4	0.75 ± 0.67	3.8 ± 0.71	7.8 ± 3.7	2.6 ± 1.7	1.8 ± 0.39
benzoic acid	5.4 ± 1.2					2.8 ± 4.9	
benzyl alcohol	0.72 ± 0.46						
dihydro-2,5-furandione	22 ± 0.09		4.2 ± 4.7		2.5 ± 3.5	6.3 ± 5.6	
dihydro-5-methyl-2(3*H*)-furanone					9.1 ± 4.7	3.0 ± 3.1	
ethyl-nitrophenol[l]					7.0 ± 1.7		
m-cresol	0.15 ± 0.03						
m-tolualdehyde		3.9 ± 3.0				6.31 ± 3.82	
m-toluic acid		9.2 ± 4.6				1.2 ± 1.0	
o-cresol	0.02 ± 0.02						
p-cresol			0.33 ± 0.35				0.29 ± 0.02
p-tolualdehyde			14 ± 16				7.1 ± 2.6
p-toluic acid			3.3 ± 4.0				0.86 ± 0.38
phenol	0.09 ± 0.01				0.19 ± +	0.04 ± 0.01	0.02 ± 0.01
sec-phenethyl alcohol					1.3 ± 0.24		
terephthaldicarboxaldehyde							0.33 ± 0.08

[a] Numbers given are percentages of the total identified mass for the particular precursor aromatic. [b] Organic tentatively identified from its mass spectra. Contribution estimated using response of 1,4-benzoquinone. [c] Organic identified by match in Wiley mass spectral library. Contribution estimated using response of 1,4-benzoquinone. [d] Organic tentatively identified from its mass spectra. Contribution estimated using response of 2,2-dimethyl-3(2*H*)-furanone. [e] Organic identified by match in Wiley mass spectral library. This organic could also be 5-ethyl-2(3*H*)-furanone. Contribution estimated using response of 5-methyl-2(5*H*)-furanone. [f] Organic identified by match in Wiley mass spectral library. Contribution estimated using response of 3-methyl-2,5-furandione. [g] Organic tentatively identified from its mass spectra. This organic could also be 5-ethyl-3-methyl-2(3*H*)-furanone. Contribution estimated using 3-methyl-2(5*H*)-furanone. [h] Organic tentatively identified from its mass spectra. Contribution estimated using 2,5-hexanedione. [i] Organic tentatively identified from its mass spectra. This organic could also be 3-ethyl-5-methyl-2(3*H*)-furanone. Contribution estimated using 5-methyl-2(5*H*)-furanone. [j] Organic matched reference in NIST mass spectral library. Contribution estimated using 5-methyl-2-nitrophenol. [k] Organic identified by match in Wiley mass spectral library. Contribution estimated using 5-methyl-2(3*H*)-furanone. [l] Organic identified by match in Wiley library. Any isomer could be possible. Contribution estimated using 2,6-dimethyl-4-nitrophenol.

ranged from 2 to 8 ppm, and initial propene mixing ratios were approximately 1 ppm. Hydrocarbon−NO_x ratios were at least 25 ppm C/ppm, a level that has been previously found to be optimal for secondary organic aerosol formation (*12*). Initial particles were also injected into the small smog chamber at concentrations up to 1000 cm^{-3}. It is important to note that, although the initial individual hydrocarbon concentrations are an order of magnitude or more above ambient urban levels, the hydroxyl radical chemistry occurring in the chamber is the same as that under ambient conditions. Hence, these mechanistic observations are expected to be valid for atmospheric conditions. The subsequent reactions of the OH−aromatic adducts are not independent of NO_2 concentrations, and in consideration of the high NO_2 levels in smog chamber experiments as compared to ambient conditions, these OH−aromatic adduct reactions are more significant than in the ambient atmosphere.

Sample Collection. Once significant secondary particulate matter had formed, as monitored by the scanning electrical mobility spectrometer (*13*), particles were collected. Sampling typically began 4−6 h into the experiment. The smog chamber was deflated through filter samplers, each operating at 10L min^{-1}. For the experiments, five samplers all containing quartz fiber filters were used. Quartz fiber filters 47 mm in diameter from Pallflex (Putnam, CT) were used. Sampling lasted from 2 to 4 h. Prior to usage, the filters were baked at 750 °C for at least 2 h. The filters were stored in glass jars with Teflon-lined lids at sub-zero temperatures immediately after collection. The storage jars were prepared prior to use by rinsing in distilled water, then twice with HPLC-grade methanol, and finally in HPLC-grade methylene chloride. The open ends of the jars were covered with foil, and the jars were baked at 550 °C for at least 4 h. The filter samplers and the Teflon-lined lids of the jars were similarly cleaned by sonication in distilled water, then in HPLC-grade methanol, and finally in HPLC-grade hexane. The sample collection procedure and the cleaning protocol with respect to handling quartz fiber filters have been adapted from the procedures of Hildemann *et al.* (*14*) and Rogge *et al.* (*15*−*19*).

Various blank filters were tested for quality assurance. One test involved extracting filters immediately after baking at 750 °C. The extraction procedure is outlined in the following section. The filters were found to contain no trace organics. Filter samples were also taken from the smog chamber on those days during which the chamber was baking. These filters of background particle loading contained trace amounts of organics, potentially identifiable as isobenzofurandione and phthalide. Phthalates are common plasticizers and are often detected as contaminants in sampling studies (*15*). It should be noted that organic vapors may absorb onto particles already collected on the filter surface. This aspect was not quantified in the present study. Compounds that are particle-bound during sampling are considered to comprise the collected aerosol in primary aerosol studies (*15*−*19*). This lack of quantification was not viewed as critical to the goal of this study of identifying organic products that are susceptible to partitioning to the particle phase. By identifying the organics, we can evaluate chemical mechanisms leading to these species. For further reference in this paper, the species identified from the extraction of particles and absorbed organic vapors on quartz fiber filters are correctly referred to as species of secondary organic aerosol.

Sample Extraction. A new extraction protocol was developed for the quantitative analysis of secondary organic aerosol on quartz fiber filters (*4*). The extraction method was optimized by recovery studies of filters impregnated with 5−50 μL of an organic standard containing an approximate concentration each of 1 mg μL^{-1} in methanol: *tert*-butyl hydroperoxide, butyl ester of nitric acid, heptanal, hexanoic acid, nonanal, 2-ethylhexyl nitrate, 2-nitro-*m*-xylene, benzoic acid, 5-nitro-*m*-xylene, undecanal, decanoic acid, pentanedioic acid, hexanedioic acid, dodecanoic acid, and tetradecanoic acid (*4*). These compounds were chosen as they have either been previously identified as gas-phase oxidation products (*9, 20*) or they have relevant functional groups, for example, nitrates and hydroperoxides. Numerous extractions of the recovery standard were performed, and no conversion of any of the species in the standard was observed. The SFE-GC/MS (supercritical fluid extraction-gas chromatograph/mass spectrometer) system does not appear to induce any reaction of the analytes. The optimal method was found to be extraction using supercritical CO_2, modified with a 10% solution of acetic acid in methanol. The addition of acetic acid was necessary for extraction of organic acids from the quartz fiber filters. The Suprex PrepMaster (Pittsburgh, PA) extraction unit and modifier pump were used. The filters were allowed to equilibrate in CO_2 at 150 °C and 420 atm for 10 min. Then the filters were extracted for 30 min with CO_2 flowing at approximately 1 mL min^{-1}. Modifier was added at a rate of 2% of the CO_2 flow rate. Analytes and CO_2 passed directly through a heated transfer line to the gas chromatograph (GC). The GC column was cryo-cooled to −30 °C, trapping the analytes in the first few meters of the column while allowing the CO_2 to vent. Once the extraction was complete, the GC stepped through its temperature program.

GC/MS Analysis. A Hewlett Packard 5890 Series II gas chromatograph and a Hewlett Packard 5989A mass spectrometer engine were used. After high-resolution chromatography using an HP-1701 60 m fused silica column (14% cyanopropyl−phenyl methyl−polysiloxane) with a film thickness of 0.25 μm and inner diameter of 0.25 mm, the MS analyses were performed by electron impact ionization. The HP ChemSystem software in conjunction with the Wiley library of organic spectra was employed to initially identify organic compounds in the samples. The species identified were later confirmed by matching retention times with authentic standards and then quantified. All standards were obtained from Aldrich Chemical Co. (St. Louis, MO) and were used without further purification.

Composition of Secondary Organic Aerosol

The compounds identified are listed alphabetically in Table 2 for all aromatic systems. The quantities measured for each compound have been normalized with respect to the total mass of identifiable species from the parent hydrocarbon. Only 15−30% of the mass that was extracted from the quartz filters and eluted through the gas chromatograph could be verified with standards. This result is typical of molecular composition studies of complex atmospheric aerosol mixtures (*15*−*19*). The unidentified fraction consists of peaks that are not specifically identifiable and the unresolved mixture emerging late in the chromatograms. The entries in Table 2 are normalized amounts expressed as a percentage; they reflect the relative contribution each compound makes to the quantifiable and identifiable SOA for the particular parent aromatic. Species detected but at a level too low to be quantified are denoted with a '+'. All species, except when noted, were verified and quantified with authentic standards. The remaining compounds were tentatively identified either with a match in a mass spectral library or by interpretation of the mass spectra. Contributions of these organics to the identifiable SOA were estimated from the response of similarly structured compounds, as noted in the footnotes to Table 2.

The distribution of products in the secondary organic aerosol reflects the results of two distinct processes: the gas-phase photooxidation of the aromatic and the subsequent partitioning of the reaction products into the particle phase. First, there is a gas-phase yield associated with each first, second, third, *etc.* generation product according to the oxidation chemistry resulting in its formation. As an example, consider benzaldehyde. Toluene reacts with OH radicals,

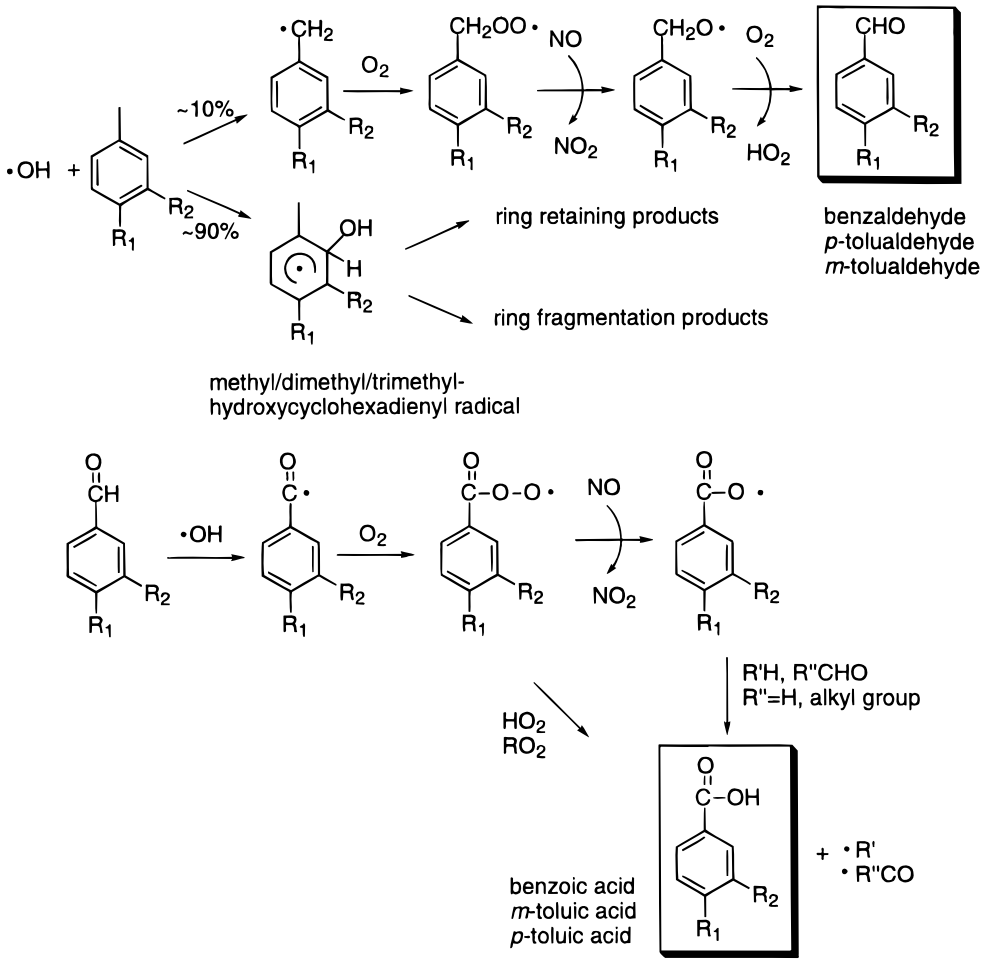

FIGURE 1. Toluene-, *m*-xylene-, *p*-xylene−OH initial reaction split and details of abstraction path. R_1, R_2 = H for toluene. $R_1 = CH_3$, R_2 = H for *p*-xylene. R_1 = H, $R_2 = CH_3$ for *m*-xylene.

with a benzaldehyde yield of approximately 10% (*9*). That is, for every 10 molecules of toluene that reacts with OH in the presence of sufficient NO_x, 1 molecule of benzaldehyde forms. Then there is another yield, or more precisely a gas/particle partitioning, associated with the benzaldehyde molecule. This partitioning may depend on physicochemical parameters, such as the compound's vapor pressure, the amount of organic aerosol present, and temperature. The overall measured contribution of a product like benzaldehyde to the measured aerosol mass reflects both its gas-phase reaction yield and its gas/particle partitioning coefficient. The aerosol mass that is identified is typically less than 1% of the total amount of reacted aromatic. Consequently, an attempt to interpret the results in Table 2 as gas-phase reaction yields is inappropriate.

Toluene. The toluene−OH reaction results in about 10% H-atom abstraction from the methyl group and 90% OH addition to the ring (*9*). The addition pathway is thought to yield ring-fragmentation products, in amounts upwards of 65% of the overall OH radical reaction (*9*). The components of toluene SOA identified and verified in the present study comprise less than 40% ring-retaining products and more than 60% of those most likely arising from ring-fragmentation pathways. The more dominant identified species in toluene SOA include 3-methyl-2,5-furandione, dihydro-2,5-furandione, 2-methyl-4-nitrophenol, 2,5-furandione, 3-methyl-4-nitrophenol, and benzoic acid. Mechanisms leading to the formation of these compounds will be discussed subsequently. The presence of relatively high vapor pressure ring-fragmentation products in SOA is consistent with the semivolatile gas/particle partitioning model in which gas-phase organics absorb into the organic particulate phase (*1*−*4*). The predominant compound identified in toluene SOA is 3-methyl-2,5-furandione, also known as citraconic anhydride, the anhydride of citraconic acid. This compound has estimated vapor pressures of 1 (1320 ppm) and 5 mmHg (6580 ppm) at 47.1 and 74.8 °C, respectively (*21*). If vapor pressure alone determines whether or not a compound is present in the particle phase, it would not be expected that 3-methyl-2,5-furandione would be an aerosol component. Another example is 2,5-furandione of which a significant amount is in the particle phase, yet its vapor pressure has been estimated to be 0.36 mmHg (470 ppm) at 35 °C (*21*). According to the gas/particle partitioning model, in order for either of these compounds to exist in the particle phase they must absorb into the organic aerosol mass. Although the presence of these anhydrides could also result from the dehydration upon heating of the corresponding dicarboxylic acids (*22*), for example, 3-methyl-2,5-furandione from citraconic acid, during supercritical CO_2 extraction, adipic acid and glutaric acid were included in the standard; no cyclization of these compounds was detected. Furthermore, since the relative humidity of the smog chamber experiments ranged from 15 to 25%, conversion of the anhydride to the corresponding acid is unlikely. The presence of these anhydrides arises largely from gas/particle partitioning.

***m*-Xylene.** Ring-fragmentation products comprise a significant portion (approximately 75%) of the SOA, with the remainder ring-retaining products. Dominant organics in the total identifiable mass include 3-methyl-2,5-furandione, *m*-toluic acid, and 2,5-furandione.

***p*-Xylene.** Organics contributing primarily to the identifiable SOA are 3-methyl-2,5-furandione, *p*-tolualdehyde, 4-methyl-2-nitrophenol, 2,5-hexanedione, dihydro-2,5-furan-

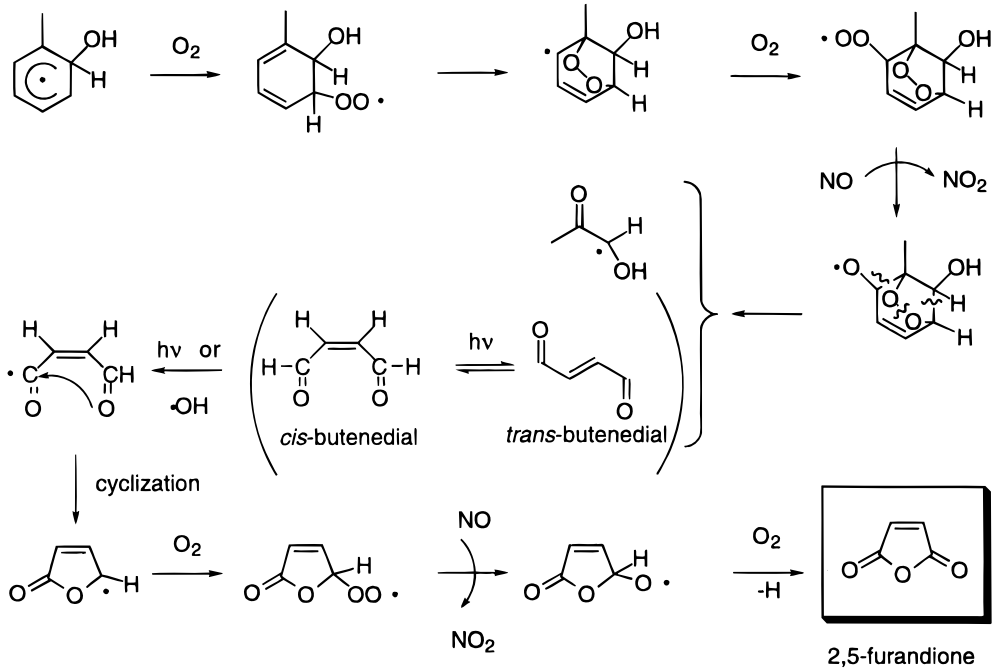

FIGURE 2. Toluene−OH pathway leading to 2,5-furandione (ref 11).

dione, and *p*-toluic acid. The contribution of 4-methyl-2-nitrophenol to SOA is uncertain, as there is significant error (>100%) in the measurement (Table 2). It is likely that artifact in one sample (of four taken) skewed the calculation of the average distribution. Hence, 4-methyl-2-nitrophenol is interpreted as a contaminant from a previous experiment.

1,2,4-Trimethylbenzene. Nearly an equal split between ring-retaining and ring-fragmentation products were identified in 1,2,4-trimethylbenzene SOA. The organics contributing significantly (greater than 5% by mass) to the identifiable SOA include 4-methylphthalic acid, 3-methyl-2,5-furandione, 3,4-dimethylbenzoic acid, 3-methyl-2,5-hexanedione, and 2,5-furandione. It should be noted that 3-methyl-2,5-hexanedione was not verified with an authentic standard but was only identified from a match with a library entry. Consequently, its identification should be viewed as provisional until verification.

Ethylbenzene. A significant portion of the organics identified likely arise from ring-fragmentation mechanisms. The species identified in decreasing order of significance are acetophenone, 3-methyl-2,5-furandione, 2,5-furandione, dihydro-5-methyl-2-furanone, benzaldehyde, 3-ethyl-2,5-furandione, and an ethyl nitrophenol. It should be noted that 3-ethyl-2,5-furandione and the ethyl nitrophenol were not verified with authentic standards but were only identified from matches with library entries.

***m*-Ethyltoluene.** Species contributing over 5% of the SOA mass are 3-ethyl-2,5-furandione, 3-methyl-2,5-furandione, 3'-methylacetophenone, 2,5-furandione, 3-ethylbenzoic acid, *m*-tolualdehyde, and dihydro-2,5-furandione.

***p*-Ethyltoluene.** Species contributing over 5% of the SOA mass are 3-ethyl-2,5-furandione, 3-methyl-2,5-furandione, 4'-methylacetophenone, *p*-tolualdehyde, and 2,5-furandione.

Toluene Photooxidation Mechanisms

Possible mechanisms leading to the toluene−OH radical products identified as SOA components are depicted in Figures 1−5. The species listed in Table 2 identified in the aerosol phase are highlighted in the mechanisms by boxes. Only mechanisms of toluene photooxidation leading to the more predominant products will be discussed. The initial OH radical attack on toluene is depicted in Figure 1, illustrating the abstraction/addition pathway split and, as noted above, the formation of benzaldehyde (*9*), which can further oxidize to benzoic acid. OH abstracts a hydrogen atom from the carbonyl group, and oxygen adds to the radical. This peroxy radical can react with RO_2 (or HO_2) to form the carboxylic acid directly, or it can react with NO to form an alkoxy radical and NO_2. The alkoxy radical can abstract a hydrogen from another toluene molecule, from a benzaldehyde molecule, or from a formaldehyde molecule to yield the carboxylic acid and to propagate the radical chain reaction. Figure 1 also outlines this suggested mechanism leading to the acid.

The addition of OH to the ring results in methyl hydroxycyclohexadienyl radicals (Figure 1), a path estimated to be 90% of the OH−toluene reaction. Most products in toluene photooxidation result from subsequent reactions of the methyl hydroxycyclohexadienyl radical, comprising both ring-retaining species and ring-fragmentation species. The OH radical can add to toluene in the *ortho*, *meta* and *para* positions, with the *ortho* position energetically favored (*23*). The methyl hydroxycyclohexadienyl radical may react with O_2 or NO_2 (*9*, *11*, *23*−*25*).

The methyl hydroxycyclohexadienyl radical reacts with O_2 to form a methyl hydroxycyclohexadienyl peroxy radical (Figure 2). OH is favored thermodynamically to add *ortho* to the methyl group on the ring, and the peroxy group can bridge as shown in Figure 2 (*23*, *26*). The resulting alkyl radical rapidly adds O_2 and reacts with NO to form NO_2 and an alkoxy radical. This alkoxy radical decomposes to form either *cis*- or *trans*-butenedial and an oxo-hydroxypropyl radical. *trans*-Butenedial has been shown to photoisomerize to *cis*-butenedial with a rate constant of $3.9 \times 10^{-4}\ s^{-1}$ (*11*). The *cis* isomer has been postulated to lose a hydrogen atom from the carbonyl group via OH radical attack or by photolysis, with subsequent O_2 addition and rearrangement to form 2,5-furandione (*11*). The details of this mechanism are outlined in Figure 2.

Of the identifiable fraction of toluene SOA, 3-methyl-2,5-furandione is the predominant species. Based on the photoisomerization and oxidation mechanism for unsaturated dicarbonyls proposed by Bierbach *et al.* (*11*), the formation of 3-methyl-2,5-furandione is consistent with that from 2-methyl-2-butenedial. Figure 3a shows the detailed mechanism to form this anhydride from the unsaturated dicarbonyl, in addition to the rearrangement mechanism to

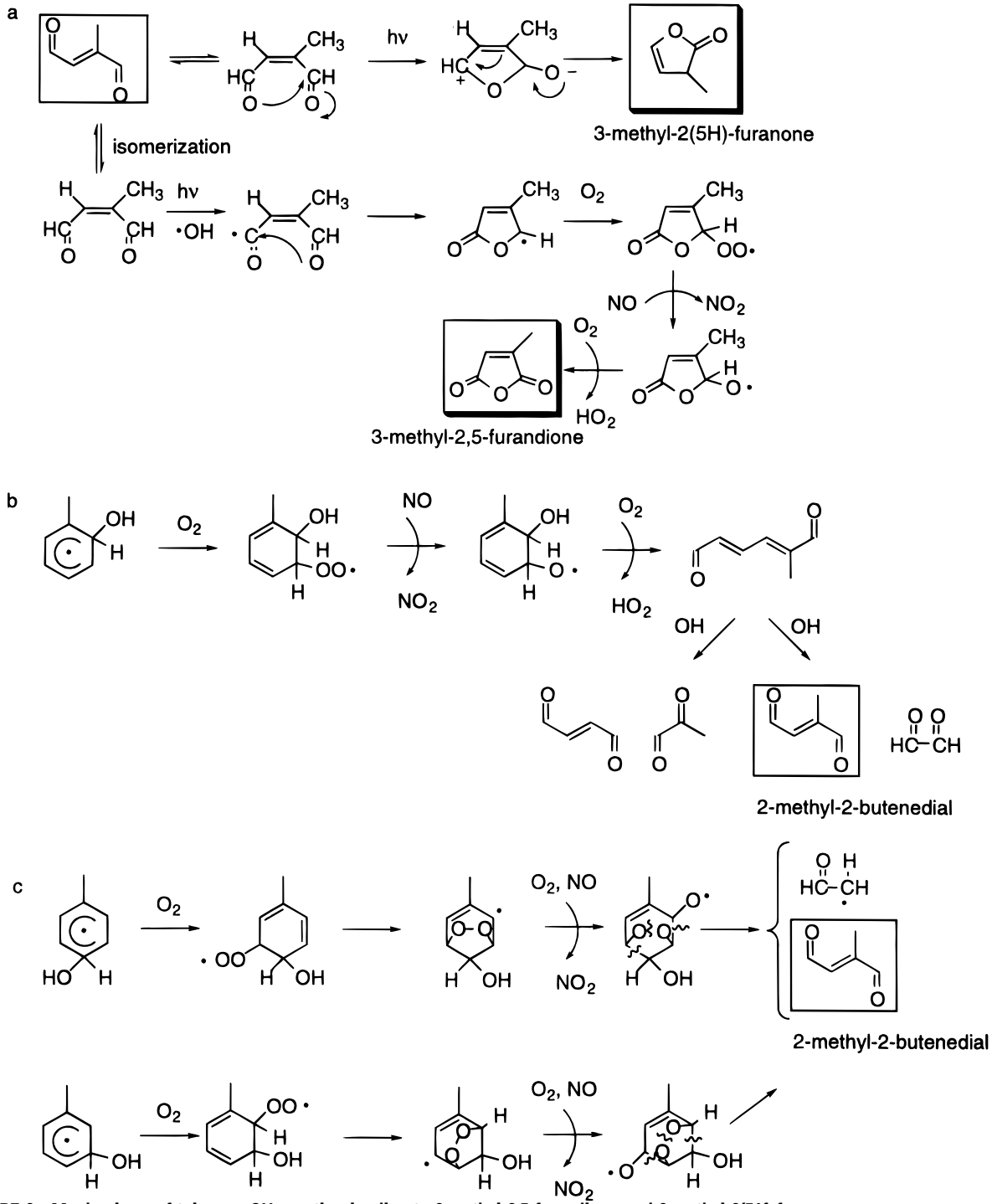

FIGURE 3. Mechanisms of toluene–OH reaction leading to 3-methyl-2,5-furandione and 3-methyl-2(5*H*)-furanone.

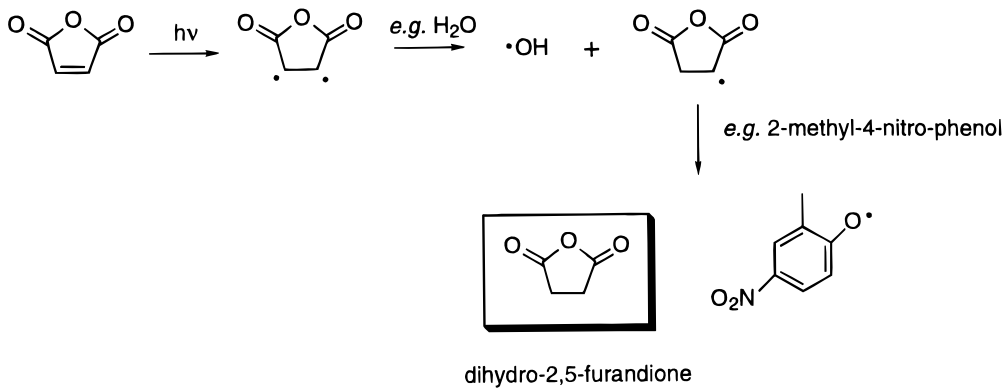

FIGURE 4. Photolytically induced mechanism from 2,5-furandione to dihydro-2,5-furandione.

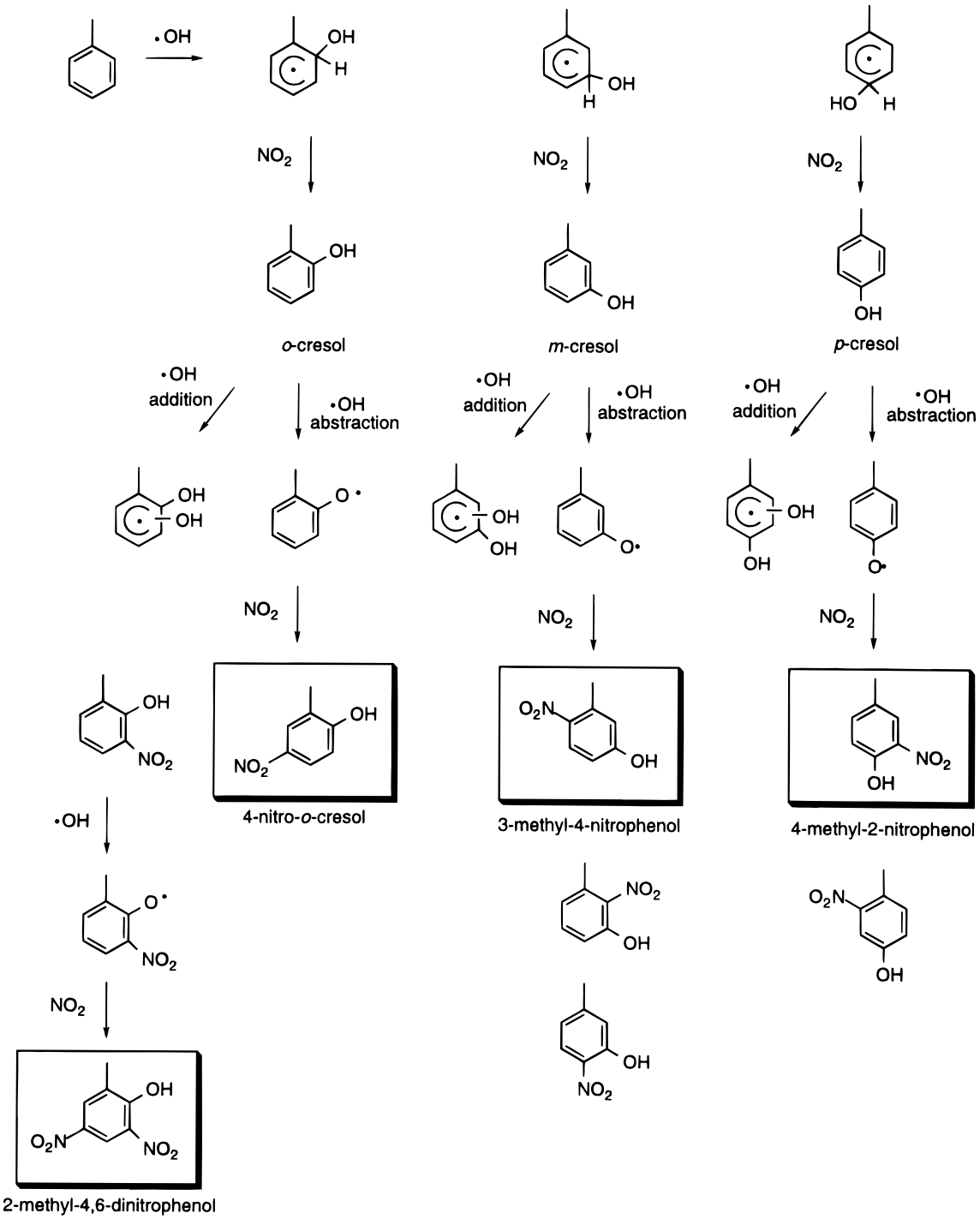

FIGURE 5. Reactions of NO_2 with the methyl hydroxycyclohexadienyl radical resulting from toluene−OH reaction leading to observed organic aerosol products.

form 3-methyl-2(5*H*)-furanone. Mechanisms to form 2-methyl-2-butenedial from OH−toluene adducts are outlined in Figure 3, panels b and c. The more likely mechanism arises from the energetically favored *ortho*-methyl hydroxycyclohexadienyl radical (Figure 3b). After the addition of oxygen, this radical cleaves to form 2-methyl-2,4-hexadienedial (*27*, *28*). Addition of hydroxyl radicals results in 2-methyl-2-butenedial. The other mechanism involves OH radical addition to toluene in the *meta* or *para* positions with further oxidation leading to a bridged peroxy alkyl radical (Figure 3c). This alkyl radical can be further oxidized and ultimately fragment to form 2-methyl butenedial and an oxygenated ethyl radical (*23*).

Significant quantities of dihydro-2,5-furandione (succinic anhydride) were detected in the toluene aerosol (Table 2). Upon first consideration, it would seem that a saturated anhydride would not result from the photooxidation of an aromatic compound, particularly since previous studies have not reported saturated compounds. Photoreduction of ketones in the solution phase is well established, and there is evidence to support intermolecular hydrogen abstraction of cyclic ethylenes after photo-excitation (*29*). Given the lack of prior evidence of succinic anhydride as a product in gas-phase toluene photooxidation, it is possible that succinic anhydride forms from the intermolecular hydrogen abstraction of 2,5-furandione in the particle phase. Water, nitrophenols, and benzoic acid in the particle phase can contribute to a slightly acidic environment in the particle, allowing facile proton (H) exchange. Figure 4 outlines a possible mechanism to produce dihydro-2,5-furandione. Once in the particle

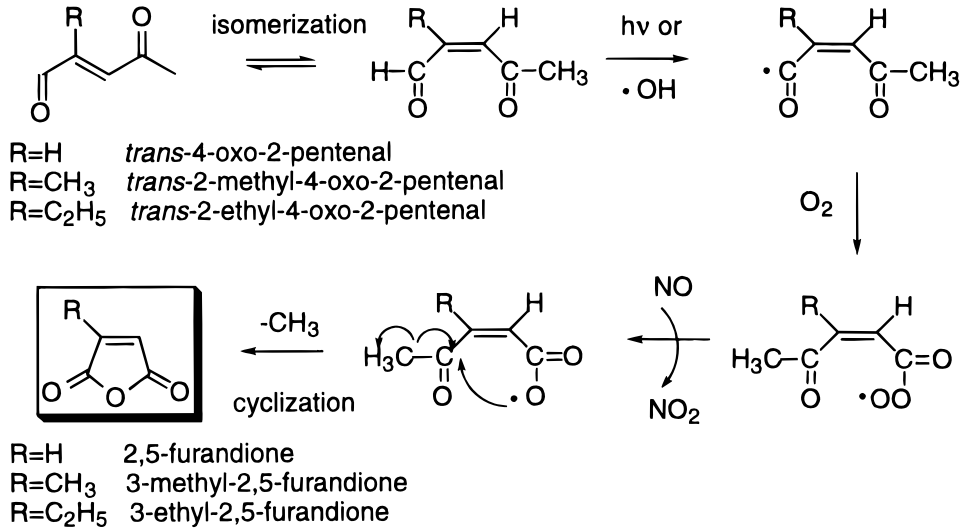

FIGURE 6. Formation of 2,5-furandione from *trans*-4-oxo-2-pentenal, formation of 3-methyl-2,5-furandione from *trans*-2-methyl-4-oxo-2-pentenal (R = CH_3), and formation of 3-ethyl-2,5-furandione from *trans*-2-ethyl-4-oxo-2-pentenal (R = C_2H_5).

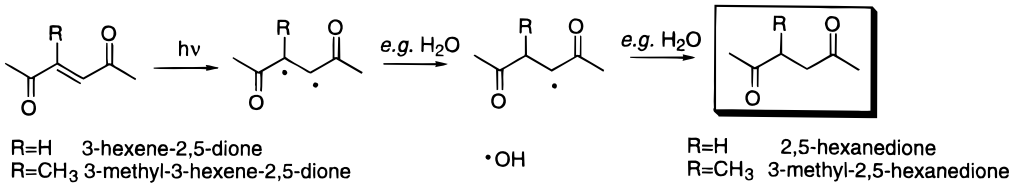

FIGURE 7. Photolytically induced mechanism from 3-hexene-2,5-dione to 2,5-hexanedione and from 3-methyl-3-hexene-2,5-dione to 3-methyl-2,5-hexanedione.

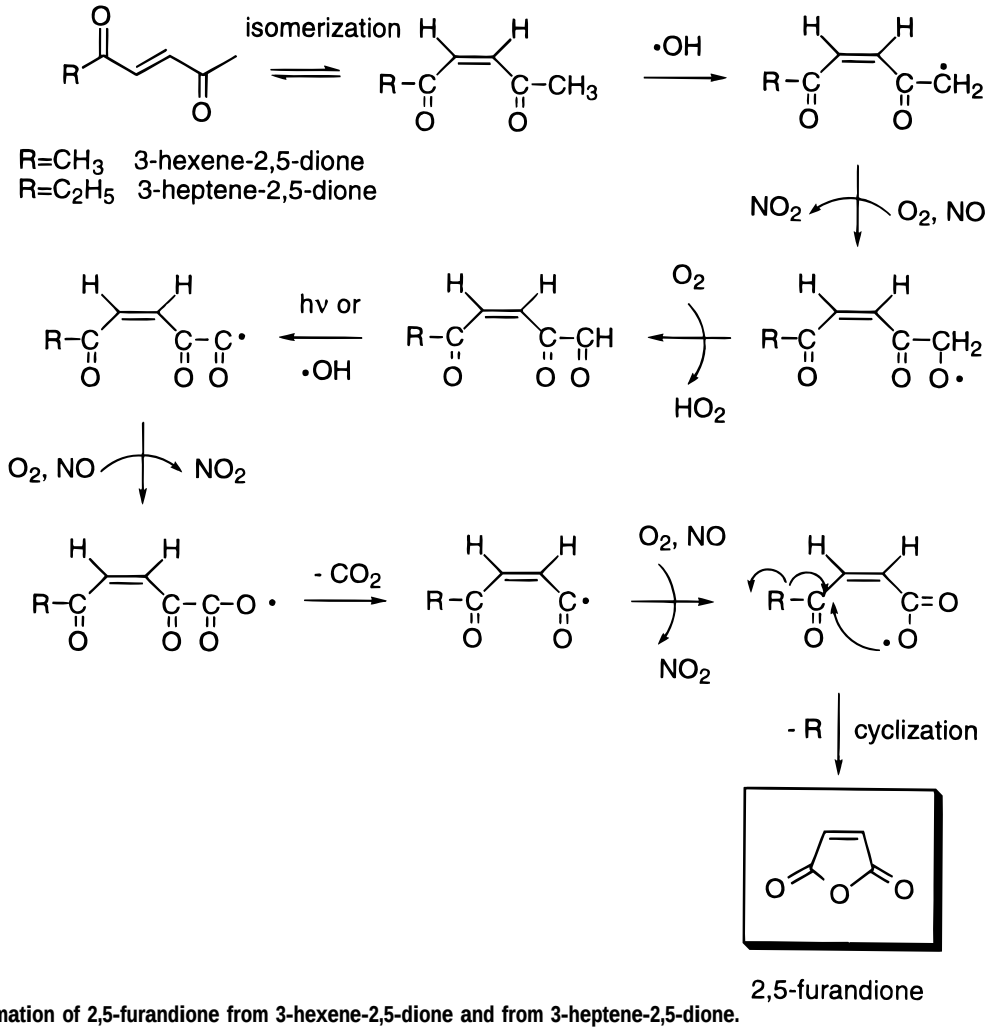

FIGURE 8. Formation of 2,5-furandione from 3-hexene-2,5-dione and from 3-heptene-2,5-dione.

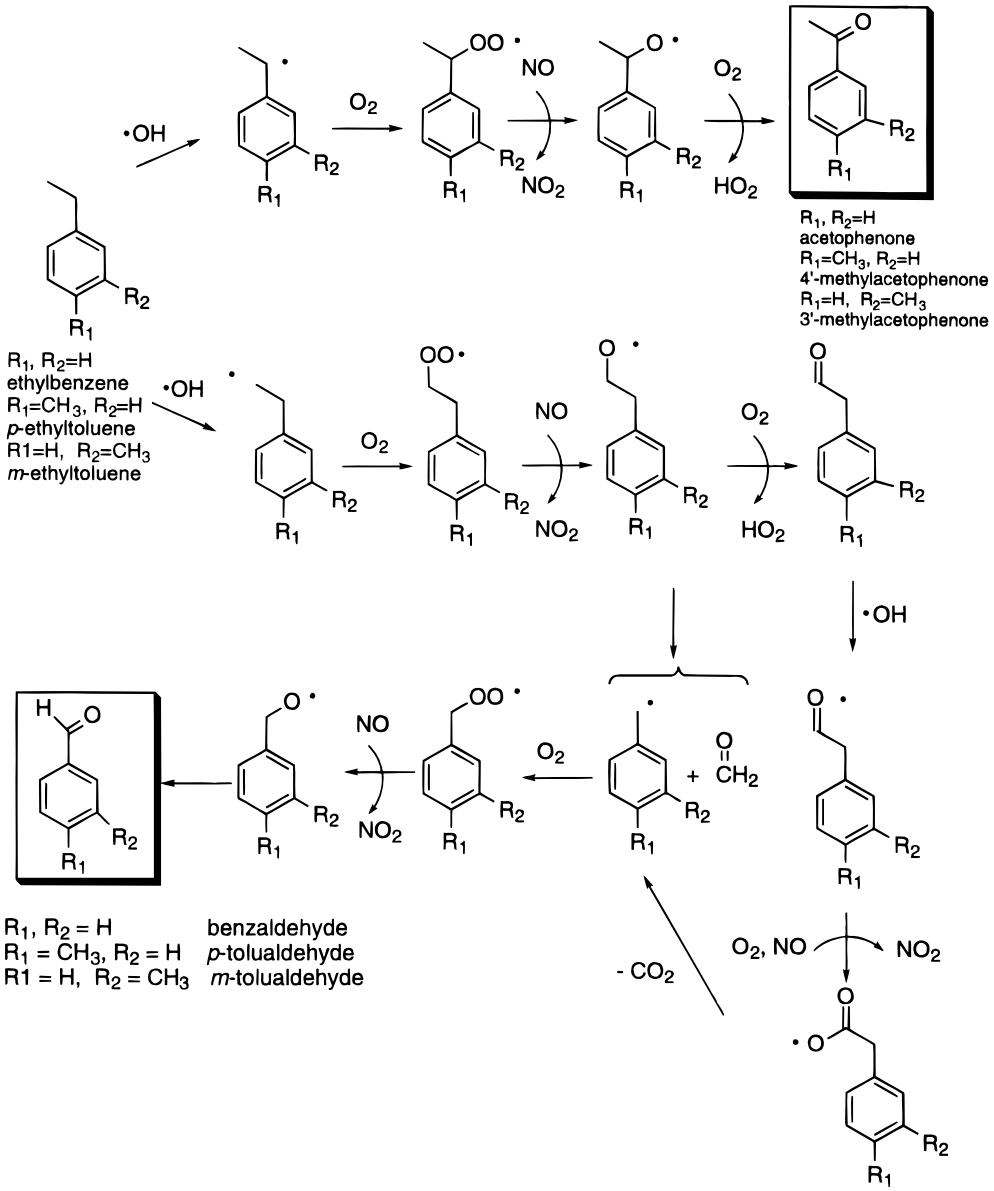

FIGURE 9. Ethylbenzene–OH pathway leading to acetophenone and benzaldehyde. *p*-Ethyltoluene–OH pathway leading to 4'-methylacetophenone and *p*-tolualdehyde. *m*-Ethyltoluene–OH pathway leading to 3'-methylacetophenone and *m*-tolualdehyde.

phase, the 2,5-furandione is photolytically excited and may break one of the double bonds to make an alkyl biradical. Upon interaction with this alkyl biradical, water or a nitrophenol will readily yield a hydrogen, resulting in an alkyl radical and a hydroxyl or phenoxy radical. The alkyl radical will abstract another H-atom from another water molecule or nitrophenol molecule to produce succinic anhydride. Because the double bond and diketone portion of 2,5-furandione is highly reactive (cf. 1,4-benzoquinone), dihydro-2,5-furandione can form.

The methyl hydroxycyclohexadienyl radical may react with NO_2, particularly in environmental chamber studies where NO_x levels are elevated, to yield the corresponding cresols (*9*). A detailed mechanism for this step is not shown in Figure 5. After the methyl hydroxycyclohexadienyl radical reacts with NO_2 to result in either *o*-, *m*-, or *p*-cresol, OH can react with the cresol to abstract an H-atom from the hydroxyl group or add to the ring (*9*). Only the abstraction pathway is shown in Figure 5. This methyl phenoxy radical can then react with NO_2 to form a variety of nitro methyl phenolic compounds. The positions of -O• and the methyl group determine where NO_2 adds to the ring. Alkyl groups and OR groups on an aromatic ring are *ortho*- and *para*-directing, with OR more strongly activating (*22*). Hence, NO_2 adds *ortho* and *para* to the oxygen in the methyl phenoxy radical. The steps leading to 2-methyl-4-nitrophenol, 3-methyl-4-nitrophenol, and 4-methyl-2-nitrophenol are outlined in Figure 5, with these identified toluene SOA products boxed. Also shown in Figure 5 are further reactions of 2-nitro-6-methylphenol with OH and NO_2 to yield 2-methyl-4,6-dinitrophenol, another species detected in toluene SOA.

m-Xylene Photooxidation Mechanisms

Three compounds (3-methyl-2,5-furandione, *m*-toluic acid, and 2,5-furandione) comprise 75% of the identified *m*-xylene SOA. The mechanism leading to *m*-toluic acid is readily extended from the toluene–OH mechanism resulting in benzaldehyde and benzoic acid. The OH abstraction pathway for *m*-xylene is shown in Figure 1, with the subsequent steps to the carboxylic acid. On the basis of *ab initio* calculations, Andino *et al.* (*23*) determined that OH adds to *m*-xylene in the *ortho* position to both methyl groups, leading to the ring-fragmentation product of 4-oxo-2-pentenal. Less favored is OH addition in the *para* and *ortho* position to both methyl groups and the subsequent oxygen addition and β-scission reaction to yield 2-methyl-2-butenedial and 2-methyl-4-oxo-

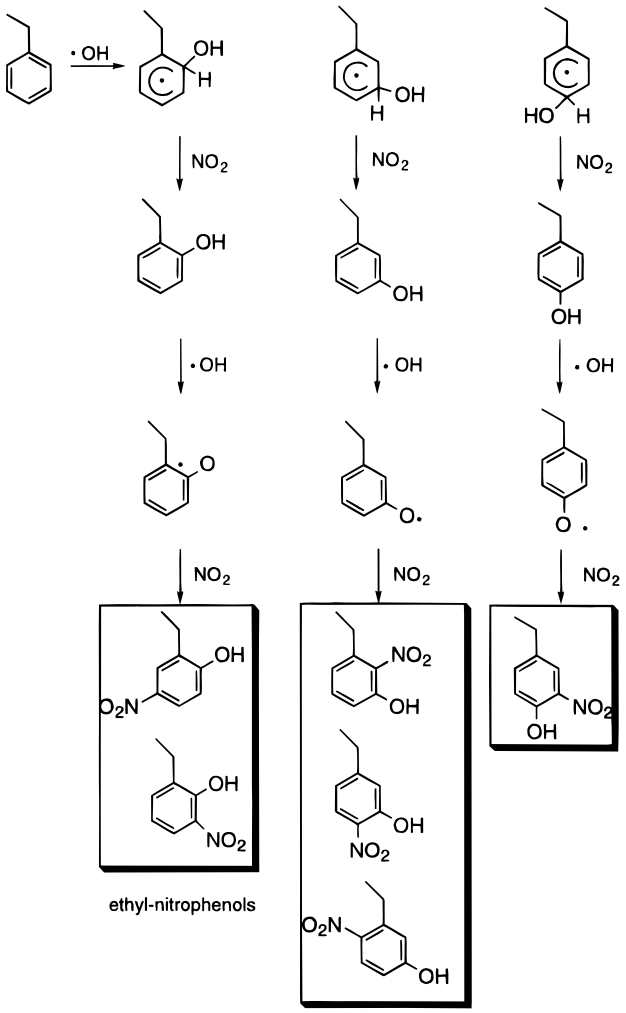

FIGURE 10. Suggested pathways of ethylbenzene–OH adduct leading to ethyl nitrophenolic compounds.

2-pentenal. Bierbach *et al.* (*11*) postulate a mechanism by which 4-oxo-2-pentenal can form 2,5-furandione. This mechanism involves the initial loss of the hydrogen adjacent to the carbonyl group by photolysis or OH abstraction. Subsequent addition of oxygen to the alkyl radical, formation of an alkoxy radical, and cyclization lead to 2,5-furandione (Figure 6). The mechanism to yield 3-methyl-2,5-furandione is outlined in Figure 3 from the photoisomerization and oxidation of 2-methyl-2-butenedial. Since 3-methyl-2,5-furandione contributes 60% by mass to the SOA, another pathway leading to this compound may exist, in addition to the ring-fragmentation leading to 2-methyl-2-butenedial. Extending the mechanism in Figure 6 to 2-methyl-4-oxo-pentenal, another pathway to 3-methyl-2,5-furandione is proposed.

p-Xylene Photooxidation Mechanisms

Similar to toluene and *m*-xylene, OH can either abstract a hydrogen from one of the methyl groups on *p*-xylene or it can add to the ring. The hydrogen abstraction pathway leads to *p*-tolualdehyde, which is identified as a significant constituent of *p*-xylene SOA. Further oxidation of *p*-tolualdehyde leads to the formation of *p*-toluic acid. The OH abstraction pathway is shown in Figure 1 resulting in the aldehyde and carboxylic acid. Andino *et al.* (*23*) also studied ring-fragmentation products from the bicyclic oxy radicals from *p*–xylene-OH addition. Because of *p*-xylene's symmetry, only 2-methyl-2-butenedial and 3-hexene-2,5-dione result. Again, as described in Figure 3 and in the previous sections, 3-methyl-2,5-furandione is formed from the photoisomerization and oxidation of 2-methyl-2-butenedial. As suggested in the toluene mechanism, dihydro-2,5-furandione may arise from a photolytic hydrogenation process of 2,5-furandione in the particle phase. Formation of 2,5-hexanedione can be analogously postulated. The 3-hexene-2,5-dione can partition into the particle phase and may be photolytically excited to break one bond of the double bond to produce an alkyl biradical. Water, *p*-toluic acid, and nitrophenols, have pK_a values of 14.9, 4.38, and approximately 8, respectively (*22*). Hence, upon interaction with this alkyl biradical, these compounds can yield a hydrogen, resulting in an alkyl radical and a hydroxyl or phenoxy radical. The alkyl radical will abstract another hydrogen from another water molecule or nitrophenol molecule to yield 2,5-hexanedione. This process is outlined in Figure 7. The other saturated organic comprising a significant portion of *p*-xylene SOA is dihydro-2,5-furandione. Its origin from 2,5-furandione has been outlined in Figure 4. Although Bierbach *et al.* (*11*) demonstrated experimentally that 2,5-furandione is produced from the UV photolysis of 3-hexene-2,5-dione, it is unlikely that this reaction occurs in the outdoor smog chamber as the relevant wavelengths are above about 290 nm. The origin of dihydro-2,5-furandione from *p*-xylene photooxidation is presently uncertain and possibly may arise from the photooxidation of 3-hexene-2,5-dione as shown in Figure 8.

1,2,4-Trimethylbenzene Photooxidation Mechanisms

The SOA resulting from 1,2,4-trimethylbenzene photooxidation contains significant amounts of ring-retaining carboxylic acids. 4-Methylphthalic acid and 3,4-dimethylbenzoic acid can result from the atmospheric oxidation of 4-methyl-

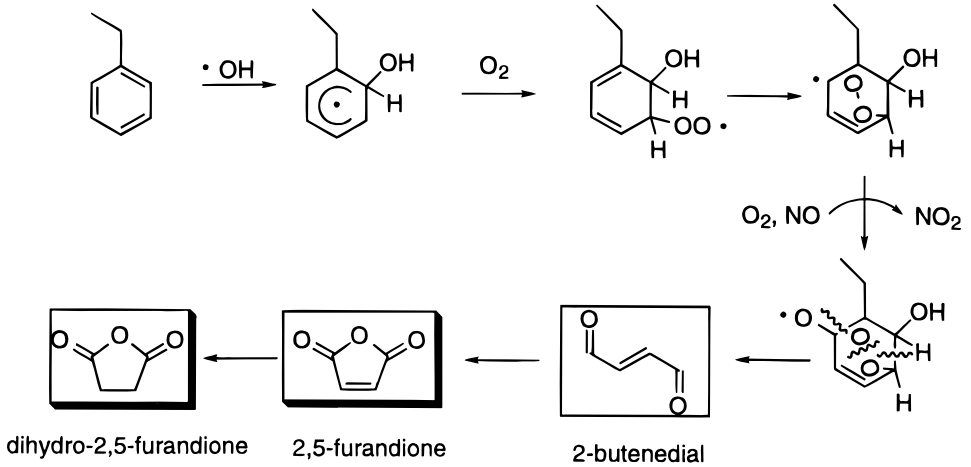

FIGURE 11. Pathway leading to 2-butenedial from ethylbenzene–OH adduct.

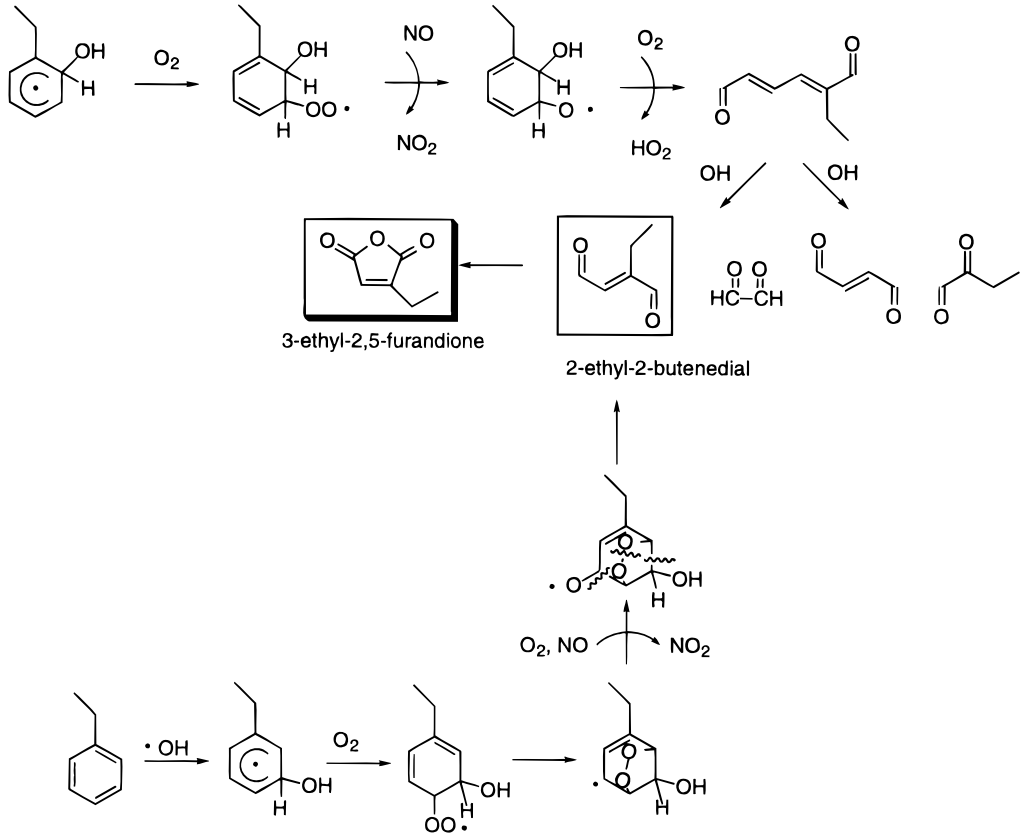

FIGURE 12. Pathway leading to 2-ethyl-2-butenedial from ethylbenzene–OH adduct.

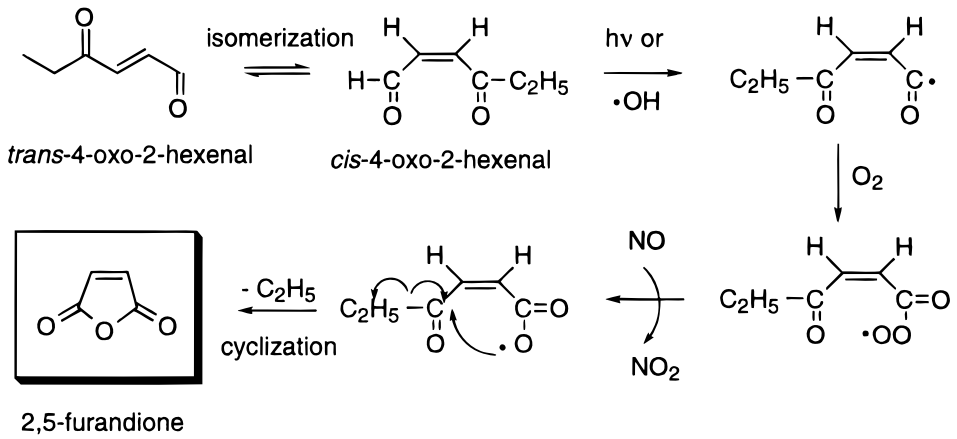

FIGURE 13. Pathway leading to 2,5-furandione from *m*-ethyltoluene photooxidation.

1,2-benzenedicarboxaldehyde and 3,4-dimethylbenzaldehyde, respectively. The substituted aldehydes arise from an OH abstraction mechanism similar to that depicted in Figure 1 for toluene, *m*-xylene, and *p*-xylene. Andino *et al.* (*23*) proposed the following gas-phase ring-fragmentation products from 1,2,4-trimethylbenzene, in decreasing order of significance: 3-methyl-3-hexene-2,5-dione, 2,3-dimethyl-2-butenedial, 3-methyl-4-oxo-2-pentenal, and 3-hexene-2,5-dione. Similar to 3-hexene-2,5-dione in the *p*-xylene photooxidation mechanisms, 3-methyl-3-hexene-2,5-dione can partition into the particle phase and may be photolytically excited to break one bond of the double bond to make an alkyl biradical. Water, a nitrophenol, or one of the carboxylic acids upon interaction with this alkyl biradical will yield a hydrogen, resulting in an alkyl radical and a hydroxyl or phenoxy radical. The alkyl radical will abstract another hydrogen from another water molecule or nitrophenol molecule to yield 3-methyl-2,5-hexanedione. This process is outlined in Figure 7. The subsequent photoisomerization and oxidation of 3-methyl-4-oxo-2-pentenal can lead to 3-methyl-2,5-furandione. Further reactions of 3-methyl-4-oxo-2-pentenal are analogous to those of 2-methyl-4-oxo-pentenal in the *m*-xylene photooxidation mechanisms (*11*). (Refer to Figure 6.) Again, the formation of 2,5-furandione from the photooxidation of 1,2,4-trimethylbenzene is presently uncertain and may arise from the photooxidation of 3-hexene-2,5-dione as shown in Figure 8.

Ethylbenzene Photooxidation Mechanisms

The photooxidation mechanisms of ethylbenzene are shown in Figures 9–12. As with the other aromatics, OH can abstract an H-atom from the alkyl group, or it can add to the ring. The abstraction route leads to the formation of acetophenone and eventually benzaldehyde. Since a secondary alkyl radical is more stable than a primary alkyl radical, the abstraction mechanism results in more acetophenone. Figure 9 suggests the steps in H abstraction from ethylbenzene. Similar to toluene–OH adduct reactions, mechanisms for ethylben-

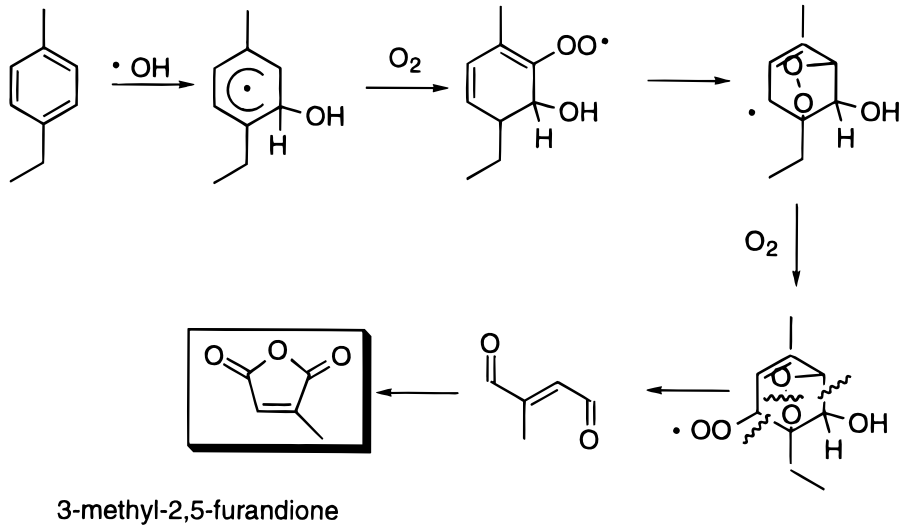

FIGURE 14. Pathway leading to 2-methyl-2-butenedial from *p*-ethyltoluene–OH adduct.

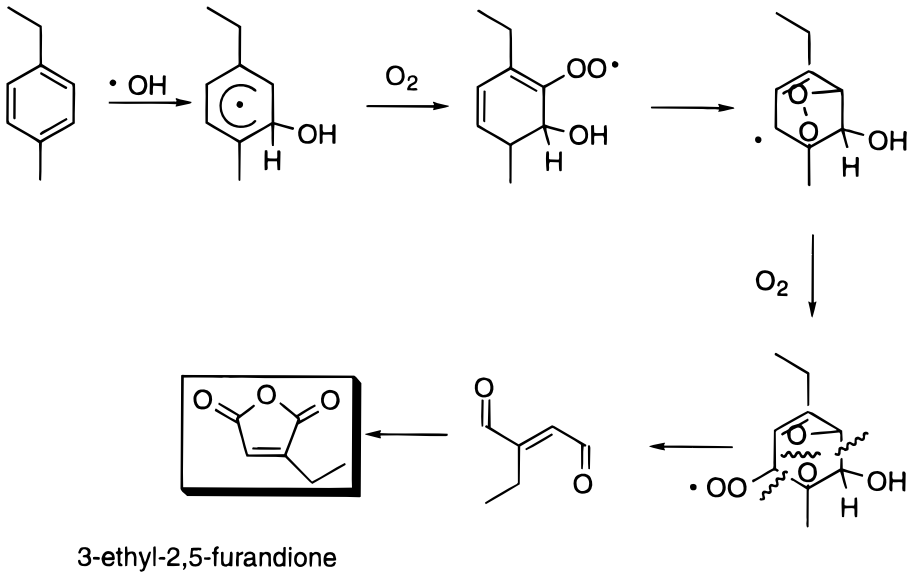

FIGURE 15. *p*-Ethyltoluene–OH adduct fragmentation pathway leading to 2-ethyl-2-butenedial.

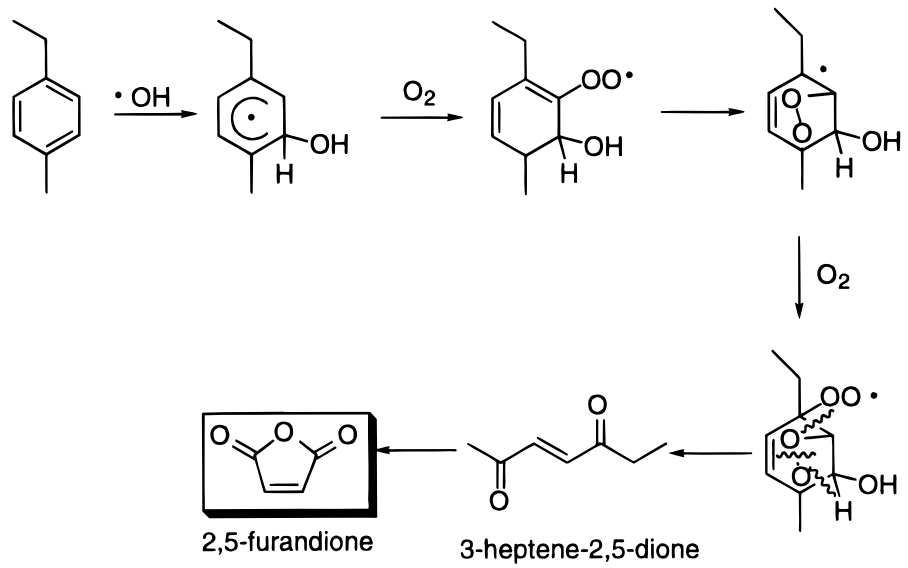

FIGURE 16. *p*-Ethyltoluene–OH adduct fragmentation pathway.

zene–OH adduct reactions leading to ethyl nitrophenols are suggested in Figure 10. Since the exact isomer was not identified, Figure 10 suggests pathways for photooxidation of ethylbenzene leading to several ethyl nitrophenolic com-

pounds. Assuming similar bicyclic oxy radicals form from ethylbenzene−OH adducts as from toluene−OH adducts, the following ring-fragmentation products can be proposed: 2-butenedial, 4-oxo-2-hexenal, and 2-ethyl-2-butenedial. The formation of 2-butenedial and 2-ethyl-2-butenedial are outlined in Figures 11 and 12, respectively, as well as the final products to which these dicarbonyls lead (*23*, *27*, *28*).

m-Ethyltoluene Photooxidation Mechanisms

For the H-abstraction pathway of *m*-ethyltoluene, OH radical attack can occur at the methyl group or the ethyl group. The probable course of H abstraction from the ethyl group is shown in Figure 9. This pathway leads to 3'-methylacetophenone and eventually *m*-tolualdehyde. Similar to the mechanism in Figure 1, 3-ethylbenzoic acid results from the H abstraction on the methyl group to form 3-ethylbenzaldehyde and subsequent oxidation of the aldehyde to the carboxylic acid. Andino *et al.* (*23*) proposed the following ring-fragmentation products from the *m*-ethyltoluene−OH adducts: 4-oxo-2-hexenal, 4-oxo-2-pentenal, 2-methyl-2-butenedial, 2-methyl-4-oxo-2-hexenal, 2-ethyl-2-butenedial, and 2-ethyl-4-oxo-2-pentenal. As illustrated in Figures 3 and 6, 2-methyl-2-butenedial, 4-oxo-2-pentenal, and 2-ethyl-4-oxo-2-pentenal lead to 3-methyl-2,5-furandione, 2,5-furandione, and 3-ethyl-2,5-furandione, respectively. These mechanisms can be extended to predict fates of the remaining dicarbonyl ring-fragmentation products. Figure 13 proposes a pathway similar to that in Figure 6, leading to 2,5-furandione from 4-oxo-2-hexenal. (4-Oxo-2-hexenal is also formed in the ethylbenzene−OH oxidation.)

p-Ethyltoluene Photooxidation Mechanisms

Hydroxyl reaction resulting in H abstraction and the products 4'-methylacetophenone and *p*-tolualdehyde is outlined in Figure 9. The OH addition pathway is adapted from the treatment of Andino *et al.* (*23*) on *p*-xylene. The proposed mechanisms leading to the ring-fragmentation products 2-methyl-2-butenedial, 2-ethyl-2-butenedial, and 3-heptene-2,5-dione are shown in Figures 14−16, respectively. These products can further react as depicted in Figures 3, 12, and 8 to form 3-methyl-2,5-furandione, 3-ethyl-2,5-furandione, and 2,5-furandione, which were detected in the *p*-ethyltoluene SOA.

Acknowledgments

This work was supported by the U.S. Environmental Protection Agency Exploratory Environmental Research Center on Airborne Organics (R-819714-01-0), National Science Foundation Grant ATM-9307603, the Coordinating Research Council (A-5-1), and the Chevron Corporation.

Literature Cited

(1) Pankow, J. F. *Atmos. Environ.* **1994**, *28*, 185−188.
(2) Pankow, J. F. *Atmos. Environ.* **1994**, *28*, 189−194.
(3) Odum, J. R.; *et al. Environ. Sci. Technol.* **1996**, *30*, 2580−2585.
(4) Forstner, H. J. L. Ph.D., California Institute of Technology, 1996.
(5) Lurmann, F. W.; Main, H. H. *Analysis of the ambient VOC data collected in the Southern California Air Quality Study*; California Air Resources Board: 1992.
(6) Stern, J. E.; Flagan, R. C.; Grosjean, D.; Seinfeld, J. H. *Environ. Sci. Technol.* **1987**, *21*, 1224−1231.
(7) Wang, S. C.; Paulson, S. E.; Grosjean, D.; Flagan, R. C.; Seinfeld, J. H. *Atmos. Environ.* **1992**, *26A*, 403−420.
(8) Izumi, K.; Fukuyama, T. *Atmos. Environ.* **1990**, *24A*, 1433−1441.
(9) Atkinson, R. *J. Phys. Chem. Ref. Data Monogr.* **1994**, *2*, 1−216.
(10) National Research Council. *Rethinking the ozone problem in urban and regional air pollution*; National Academy Press: Washington, DC, 1991.
(11) Bierbach, A.; Barnes, I.; Becker, K. H.; Wiesen, E. *Environ. Sci. Technol.* **1994**, *28*, 715−729.
(12) Zhang, Z.-H.; Shaw, M.; Seinfeld, J. H.; Flagan, R. C. *J. Geophys. Res.* **1992**, *97*, 20717−20729.
(13) Wang, S. C.; Flagan, R. C. *Aerosol Sci. Technol.* **1990**, *13*, 230−240.
(14) Hildemann, L. M.; Markowski, G. R.; Cass, G. R. *Environ. Sci. Technol.* **1991**, *25*, 744−759.
(15) Rogge, W. F.; Hildemann, L. M.; Mazurek, M. A.; Cass, G. R.; Simoneit, B. R. T. *Environ. Sci. Technol.* **1991**, *25*, 1112−1125.
(16) Rogge, W. F.; Hildemann, L. M.; Mazurek, M. a.; Cass, G. R.; Simoneit, B. R. T. *Environ. Sci. Technol.* **1993**, *27*, 636−651.
(17) Rogge, W. F.; Hildemann, L. M.; Mazurek, M. A.; Cass, G. R.; Simoneit, B. R. T. *Environ. Sci. Technol.* **1993**, *27*, 1892−1904.
(18) Rogge, W. F.; Hildemann, L. M.; Mazurek, M. A Cass, G. R.; Simoneit, B. R. T. *Environ. Sci. Technol.* **1993**, *27*, 2700−2711.
(19) Rogge, W. F.; Hildemann, L. M.; Mazurek, M. A.; Cass, G. R.; Simoneit, B. R. T. *Environ. Sci. Technol.* **1993** *27*, 2736−2744.
(20) Paulson, S. E.; Seinfeld, J. H. *Environ. Sci. Technol.* **1992**, *26*, 1165−1173.
(21) Jordan, T. E. *Vapor pressures of organic compounds*; Interscience Publishers, Inc.: New York, 1954.
(22) Streitwieser A., Jr.; Heathcock, C. H. *Introduction to Organic Chemistry*; Macmillan Publishing: New York, 1976.
(23) Andino, J. M.; Smith, J. N.; Flagan, R. C.; Goddard, W. A., III; Seinfeld, J. H. *J. Phys. Chem.* **1996**, *100*, 10967−10980.
(24) Goumri, A.; Pauwels, J.-F.; Sawerysyn, J.-P.; Devolder, P. *Chem. Phys. Lett.* **1990**, *171*, 303−308.
(25) Goumri, A.; Pauwels, J.-F.; Devolder, P. *Can. J. Chem.* **1991**, *69*, 1057−1064.
(26) Jeffries, H. E.; Yu, J.; Bartolotti, L. *Abs. Pap. Am. Chem. Soc.* **1995**, *210*, 15.
(27) Hoshino, M.; Akimoto, H.; Okuda, M. *Bull. Chem. Soc. Jpn.* **1978**, *51*, 718−724.
(28) Bartolotti, L. J.; Edney, E. O. *Chem. Phys. Lett.* **1995**, *245*, 119−122.
(29) Turro, N. J. *Modern Molecular Photochemistry*; Benjamin/Cummings Publishing Company Inc.: Menlo Park, 1978.

Received for review June 19, 1996. Revised manuscript received January 16, 1997. Accepted January 23, 1997.[⊗]

ES9605376

[⊗] Abstract published in *Advance ACS Abstracts*, April 1, 1997.